ijlpr 2022; doi 10.22376/ijpbs/lpr.2022.12.3.L23-36

International Journal of Life science and Pharma Research

ISSN 2250-0480

Research Article

ZnO Nanosperes for Better Environment

CdS Coated Mn Doped ZnO Nanospheres as Textile Catalyst: Fabrication, Physicochemical Techniques and Dye Removal Under Natural Light

K. Sivaranjani[1,2] S. Sivakumar[3] and J. Dharmaraja[4]*

[1]*Department of Chemistry, Periyar University, Salem-11, Tamil Nadu, INDIA*
[2]*Department of Chemistry, Government Arts College, Selem-7 Tamil Nadu, INDIA*
[3]*Department of Chemistry, E.R.K Arts and Science College, Dharmapuri, Tamil nadu, INDIA*
[4]*Department of Chemistry, Arignar Anna Government Arts and Science College, Attur, Tamil Nadu, INDIA*

Abstract: ZnO as a promising photocatalyst has gained much attention for the removal of organic pollutants from water. However, the main drawbacks of the relatively low photocatalytic activity and high recombination rate of photo excited electron-hole pairs, restrict its potential applications. Promoting the spatial separation of photo excited charge carriers is of paramount signi? cance for photocatalysis, because the dierence in the band positions make the potential gradient at the composite boundary. In this work, our aim is to enhance the photocatalytic efficiency of CdS coated Mn doped ZnO nanospheres under solar light irradiation. Objectives in this work are, to fabricate the CdS coated Mn doped ZnO nanospheres by a simple ethanolic dispersion method, and its applied for testing the photocatalytic activity of methylene blue (MB) dye. The fabricated binary composites were analyzed with different physicochemical techniques like PXRD, SEM with EDX, UV-DRS, PL and TEM. The photocatalytic degradation results have revealed that, the CdS coated Mn doped ZnO nanospheres exhibits admirable activity toward the photocatalytic degradation of the MB. The remarkably enhanced photocatalytic activity of CdS coated Mn doped ZnO nanospheres can be interpreted in terms of lots of active sites, which efficiently separate the photo generated electron and holes. A plausible mechanism is also elucidated via active species trapping experiments with various scavengers, which indicating that the photo generated O^{2-} and. OH radicals play a crucial role in photo degradation reactions under visible light irradiation. This work suggests that, the rational design and construction of heterostructures is powerful for developing highly efficient, and reusable visible-light photocatalysts for environmental purification and energy conversion. The enhanced photo degradation activity indicates the potential of the nanocomposite for the treatment of organic pollutants from the textile wastewater.

Keywords: CdS/Mn doped ZnO nanocomposites; Methylene Blue dye; Solar light;Dye degradation; TEM analysis

***Corresponding Author**

Dr. J. Dharmaraja , Department of Chemistry, Arignar Anna Government Arts and Science College, Attur, Tamil Nadu, INDIA

Received On 07 May 2022
Revised On 27 May 2022
Accepted On 02 June 2022
Published On 01 July 2022

Funding This research did not receive any specific grant from any funding agencies in the public, commercial or not for profit sectors.

Citation K. Sivaranjani; S. Sivakumar; J. Dharmaraja , CdS coated Mn doped ZnO nanospheres as textile catalyst: Fabrication, physicochemical techniques and dye removal under natural light.(2022).Int. J. Life Sci. Pharma Res.12(3), L23-36 http://dx.doi.org/10.22376/ijpbs/lpr.2022.12.3.L23-36

1. INTRODUCTION

The world is highly concerned about water pollution and this problem can be controlled by wastewater treatment, using low cost and environmental friendly processing techniques.[1] There are many effective processes for the treatment of wastewater, such as carbon adsorption, chemical precipitation, evaporations, ion exchange, membrane, fenton, ozonation, photocatalysis and the biological treatment.[1-3] Out of these processes, photocatalysis is one of the viable and commonly investigated process, which is very effective for the elimination of dyes, pharmaceuticals, paper industry wastes, petrochemicals and inorganic pollutants from wastewater. [4-8] The beauty of the photocatalysis is its potential to use sunlight, as a source of energy for wastewater treatment instead of using expensive reductants or oxidants.[9-11] Unlike to conventional wastewater treatment processes, the photocatalysis process results in the complete mineralization of the pollutant into harmless products like salts, CO_2 and H_2O in ambient environment.[12] As for as the photocatalysis is concerned, the semiconducting titanium oxide (TiO_2) is the extensively used catalyst for the decontamination of water and air.[13] The advantage of ZnO over the TiO_2 is that the ZnO has wide range of absorption in the solar spectrum, while the TiO2 absorbs in UV region only .[14] Due to its low cost and wide band gap (3.37 eV) , the ZnO is emerging as a most suitable alternative of TiO_2. [15] In certain cases the ZnO exhibits higher photocatalytic activity and quantum efficiency than TiO_2. Moreover, in addition to photoassisted reactions, the ZnO is also used for anti-bacterial and self-cleaning activities.[16] Though, ZnO, TiO_2 and other comparable photo-catalyst under the UV-light have ability to degrade organic pollutant only. This happens because of photo-catalysts' wide band gap, which got activated only under UV-light irradiation.[17] Therefore, on a broad scale, the utilization of such photo-catalysts may results in low photo-electronic transition efficiency as the UV-light consists only 4–5% of the solar spectrum. Thus, by considering the environmental pollution and energy conservation issues, it is essential to develop highly efficient visible light-driven photo-catalysts. Doping and nano composition of metal oxides have been considered as interesting ways of modification. The doped metal oxides have shown excellent properties in photo-catalysis. Doping is the source of modification in the features and properties of nanomaterials. To meet the cumulative demands of various applications, the nanocomposites and doping generally play an important role to improve the various properties of nanomaterials (metal oxides).[18] These properties include size reduction and surface area enhancement of nanostructured metal oxides. Moreover, the tuning of band gap-energy and shifting of absorption in the visible region, through nanocomposites and doping enhances the solar photocatalytic properties. Likewise, Mn doped ZnO nanoparticles have got substantial attention as promising photocatalysts, with enhanced photocatalytic efficiency over pristine ZnO and other transition metal-doped ZnO nanoparticles.[19,20] In order to enhance the absorption of light and provide effective charge transport, combinations of ZnO-CdS nanocomposites[21]have been exploited for the photocatalytic applications. These morphologies have various advantages, such as dimensional anisotropy, due to which the maximum number of charge carriers resides at the surface of nanorods and flow of charge along the nanorod occurs. It also facilitates high charge separation and reduced recombination resulting in high photoactivity.[22] CdS is a transition metal sulfide with a band gap of 2.4 eV with a high optical absorption coefficient.[23] Many reports suggest that the enhancement in photocatalytic activity in the visible region is due to the formation of binary composites e.g. ZnO-CdS,[24] Nanocomposites possess numerous benefits, such as high charge separation, substrate for heterogeneous nucleation, high charge carrier mobility, and increased life time of charge carrier etc. In industry, the remediation of water from MB is a major problem, as failure to remove it, has led to hazards in living organisms and the environment. Recently, various techniques for MB removal in aqueous media have been developed such as adsorption,[26] biosorption mechanism membrane, Fenton [25] and photocatalytic process. Most of the normal techniques for MB removal have limitations, as they result in secondary pollutants like adsorption and biosorption mechanisms, or they are expensive such as the membrane process. However, the photocatalytic technique for the degradation of hazardous substances becomes significant,[27] due to its unique advantages without producing secondary pollutants. Some of the photocatalytic degradation of MB dye with different types of light source are listed below. Au-ZnO - UV irradiation [28], ZnO/GO - Mercury vapor lamp [29], ZnO/$GdCoO_3$-Visible light [30] ZnO-SnO2 nano-cubes - UV irradiation NA [31] Ag-ZnO-Graphene - UV irradiation NA [32], GP-ZnO-NCs - UV irradiation NA [33], Fe-Co-ZnO - Sunlight [34] From the background discussion, we have selected CdS/Mn-doped ZnO binary photocatalyst for the degradation of methylene blue dye. The CdS/Mn-doped ZnO binary nanospheres were developed by polar solvent dispersed method. The prepared samples were characterized by XRD, SEM, TEM, EDX, UV-visible and PL spectroscopy. Photocatalytic degradation performance was evaluated on removal of methylene blue dye.

2. MATERIALS AND METHODS

2.1 Chemicals used

Methylene blue (MB) (Mark, Germany, dye content 85%) was used for photocatalytic degradation studies.
Chemical formula: $C_{16}H_{18}ClN_3S$
Molecular weight: 319.85 g/mol
Water solubility: 43.6 g/L in water at 25 °C
λ_{max}: 668 nm

Methylene Blue (Phenothiazin- 5-ium, 3,7-bis(dimethylamino)-, chloride)

Zinc chloride (98%), Sodium bica rbonate (99%) and Copper acetate (GR), Nickel chloride (GR) were supplied by Merck India Pvt. Ltd; dye solutions for photocatalytic studies were prepared in double distilled water. NaOH and HCl were used for modifying the pH of the solutions. Isopropanol,

benzoquinone and ammonium oxalate used as scavengers in deduction of active species measurement.

2.2 Preparation of Mn- doped ZnO nanopowder

In the preparation of Mn - doped ZnO nanopowder, 10 g of zinc chloride were dissolved in 100 ml of double distilled water.[35] To that solution, 6.2 g of sodium bicarbonate was then added in portions with vigorous stirring for several minutes. The precipitate formed was washed several times with distilled water to remove NaCl formed. Added 0.07mol % of manganese acetate completely washed the precipitate to the suspension. The precipitate was then dried at 100°C to remove the water. The solid obtained after drying was grinded in an agate mortar and pressed into a ceramic crucible. The material was calcined at 500°C for 4 hrs. The undoped ZnO was synthesized in the same procedure without adding dopant materials**.**

2.3 Synthesis of Cadmium sulphide[36]

CdS was synthesized by ultrasonification method. Required amount of sodium sulfide solution was slowly added into the cadmium chloride solution and stirred vigorously for 8 h. The stirred solution was left aging for another 4 h to get the product. Furthermore, it was ultrasonicated with water and transferred into 100 ml Teflon lined autoclave kept in 24 h at 180 °C. Finally, the yellow color precipitate was washed several times with ethanol and distilled water and the product was dried at 100 °C for 10 h for further characterization.

2.4 Preparation of CdS/Mn-doped ZnO binary nanospheres[37]

In the preparation of 2 wt % CdS/Mn-doped ZnO binary nanospheres, 0.02 g of CdS was first dispersed in 40 ml of ethanol, to that suspension, 0.2750 g of oxalic acid was added, and the mixture was stirred in a magnetic stirrer to form a homogeneous suspension. To that suspension, 0.98 g of Mn-doped ZnO nanopowder was added, and the stirring was continued for 12 hours and then the suspension was dried and subsequently annealed at 300°C for 3 hours in a muffle furnace. The Mn-doped ZnO nanopowder with 4, 6, 8 and 10 wt % of CdS were prepared by varying its ratios as in a same method and labeled as CMZ-2, CMZ-4, CMZ-6, CMZ-8 andCMZ-10 respectively.

2.5 Photocatalytic degradation of CdS/Mn-doped ZnO binary nanospheres

All the photocatalytic experiments were performed under natural sunlight on clear sky days during the period of January to March-2022. In a typical experiment, 50 ml of dye solution (concentration 50 mg l^{-1}) was taken with 50 mg of photocatalyst in a 250 ml glass beaker. Then the dye solution was kept in direct sunlight with continuous aeration and the concentration of the dye remains was measured periodically by measuring its light absorbance at the visible λ_{max} by using Elico SL- 171 Visible spectrophotometer. In order to avoid the variation in results due to fluctuation in the intensity of the sunlight, a set of experiments have been carried out simultaneously. Oxidant combined photocatalytic degradation process were also done as mentioned method. For pH studies the pH of the dye solutions were modified to different values (3, 5, 7, 9 and 12) by using 0.1M HCl and NaOH solution.

2.6 Characterization of Photocatalyst

X-ray powder diffraction (XRD) patterns of the photocatalysts were recorded on a Philips X'pert-MPD diffractometer in the 2h range 20°–80° using Cu Ka radiation (MRL 1012, 1032 and CNSI (Elings Hall) 1409, California, USA). The phase structure of the products was determined by comparing the experimental X-ray powder patterns to the standard compiled by the Joint Committee on Powder Diffraction and Standards (JCPDS). For morphological study of catalysts, Scanning Electron Microscopy was done by ULTRA55 FESEM, Carl Zeiss. Samples for SEM were prepared by dispersing a very small amount of catalyst in absolute ethanol by ultrasonication for 10 min. The dispersed sample was dropcasted on silicon wafers. The samples were kept under vacuum/desiccator for 12 h. Before imaging, gold sputtering was done on the samples using Quorum sputtering. Transmission electron microscopy was done by using Tecnai F30 operated at 180 kV. Samples for TEM were prepared by dispersing the catalyst in isopropanol using ultrasonication for 10 min and drop casted on Cu grid. Samples were kept under vacuum for 24 h. Diffused reflectance spectroscopic (DRS) analysis was done using solid state UV-visible spectrophotometer (Perkin Elmer, Lambda 35). Photoluminescence (PL) spectra were obtained using a photoluminescence detector (Perkin Elmer) with excitation wavelength of 325 nm.

3. RESULT AND DISCUSSION

3.1 Characterization of Photocatalysts

3.1.1 X-ray diffraction studies

The powder XRD patterns of nano ZnO, pure CdS, 0.007 mol% Mn- doped ZnO nanopowder, 6 wt% CdS/Mn-doped ZnO and 8 wt% CdS/Mn-doped ZnO binary nanospheres were shown in Fig 3.1. The ZnO samples were identified by XRD pattern as a single phase containing wurtzite crystal structure (JCPDS card nos.: 89-1397; 89-0511; 36-1451). 0.007 mol% Mn doped ZnO nanopowder shows intense diffraction pattern in the same respective wurtzite plane. The high intensity of the peaks indicates that Mn doped ZnO nanopowders are of high crystallinity.[38] The CdS crystal structure also exactly matches the JCPDS card no.89-2944. CdS/Mn doped ZnO nanosphere (4wt%) shows wurtzite phase and some important peaks of CdS. Its represent CdS coupled in the Mn doped ZnO surface. The CdS content increases (8wt%) the crystalline behavior of CdS/Mn doped ZnO nanospheres was increased. No other diffraction peaks were observed in this pattern, indicating that the CdS and ZnO phase occurred during the synthesis process.

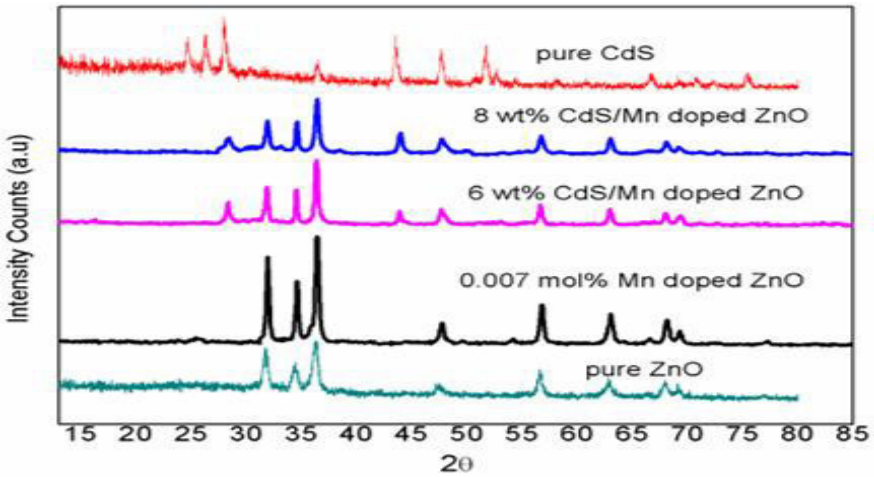

Fig 3.1XRD patterns of nano ZnO, pure CdS, 0.007 mol% Mn- doped ZnO nanopowder, 8wt% CdS/Mn-doped ZnO binary nanospheres and 10 wt% CdS/Mn-doped ZnO binary nanospheres

3.1.2 SEM analysis of the photocatalysts

Fig 3.2 demonstrate the SEM images of nano ZnO, pure CdS, 0.007 mol% Mn- doped ZnO nanopowder, 8 wt% CdS/Mn-doped ZnO binary nanospheres and 10 wt% CdS/Mn-doped ZnO binary nanosphere.It was clear from the obtained images, that the particle size of all the synthesized samples lied in the nanometer range with characteristic geometry. It was observed that ZnO nanoparticles (Fig. 3.2 a)exist in the rice-like surface structure. Pure CdS SEM image (Fig.3.2 b) shows small granular particles dispersed with an agglomerated surface. Fig 3.2 c indicates that Mn doped ZnO nanopowder have nanosized blunder particle morphology. Addition of CdSon Mn doped ZnO nanopowder (Fig 3.2 d and e) has might shows significant effect in the focused applications due to the particles highly dispersed and small particle size and particularly this weight ratio (8wt%) binary nanospheres shows small size sphere like structure. It is presumed that, the concentration of CdS as a coupling precursor played a key role in the formation of the peculiar morphology of spheres. From this study 8 wt% CdS/Mn-doped ZnO binary nanospheres suitable for solar light photocatalytic degradation.

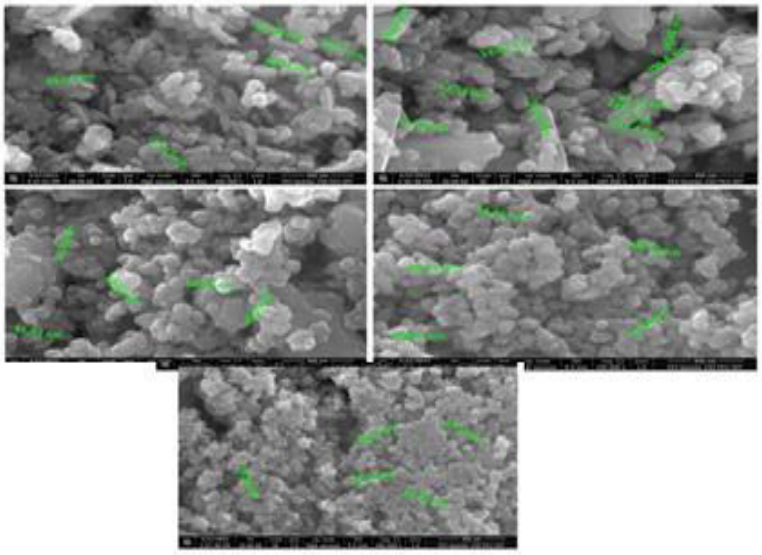

Fig 3.2 SEM micrograph of nano ZnO, pure CdS, 0.007 mol% Mn- doped ZnO nanopowder, 8 wt% CdS/Mn-doped ZnO binary nanospheres and 10 wt% CdS/Mn-doped ZnO binary nanospheres

3.1.3 Elemental composition analysis

Fig 3.3 represents the EDS spectra of the CdS/Mn doped ZnO nanosphere. The weight percentage of Zn, O, Cd, S and Mn elements in the synthesized nanomaterials are also in the Figure. **The** EDS spectra of CdS/Mn doped ZnO nanosphere, which contains 32.8 wt% of Zn, 27.2 % of Cd, O 19.2%, S 5.5 % and 4.9 wt% of Mn. These results indicate a higher amount of ZnO present than the CdS. The EDS report that CdS/Mn doped ZnO nanosphere consists of considerable amount of major components (Zn, Cd, O, Mn and S) elements in samples with some impurities like Na, C and K.[39] Finally the EDS result concluded, there are no unwanted impurities present in the prepared samples

.

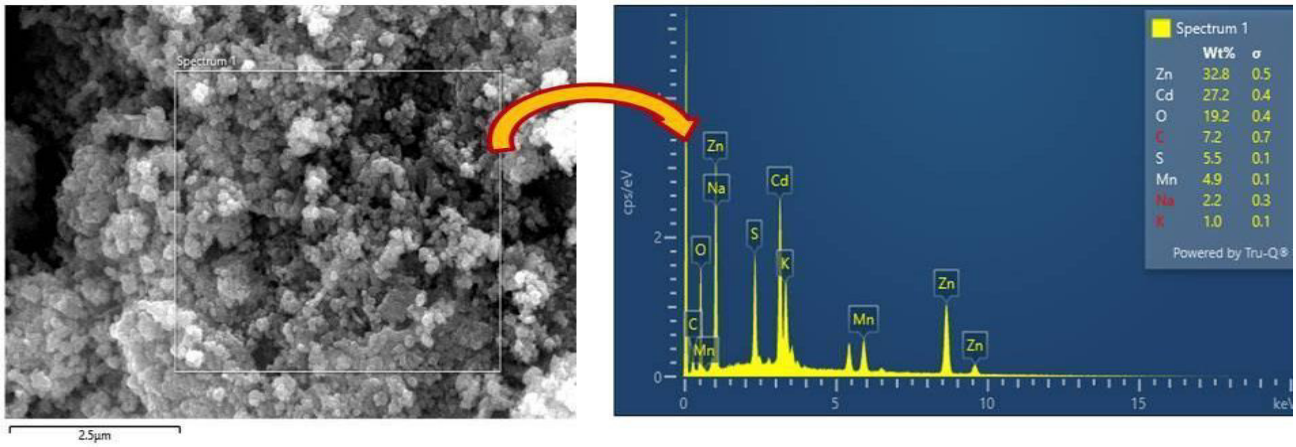

Fig 3.3 EDS spectra of CdS/Mn doped ZnO nanospheres

3.1.4 Surface particle structure analysis

Fig. 3.4a shows that the overall structure of the photocatalyst and its presented a spherical and rod like structure. Mn, CdS and ZnO are stacked in close contact with each other. The dense small spherical dot in Fig. 3.4 b represents the CdS covered uniformly to the Mn doped ZnO nanopowder surface. From the TEM results, the CdS/Mn doped ZnO nanospheres were successfully composited. [40]From the results of the fringe analysis in Fig. 3.4c, it can be seen that the lattice spacing of the ZnO (002) crystal plane are 0.26 nm.

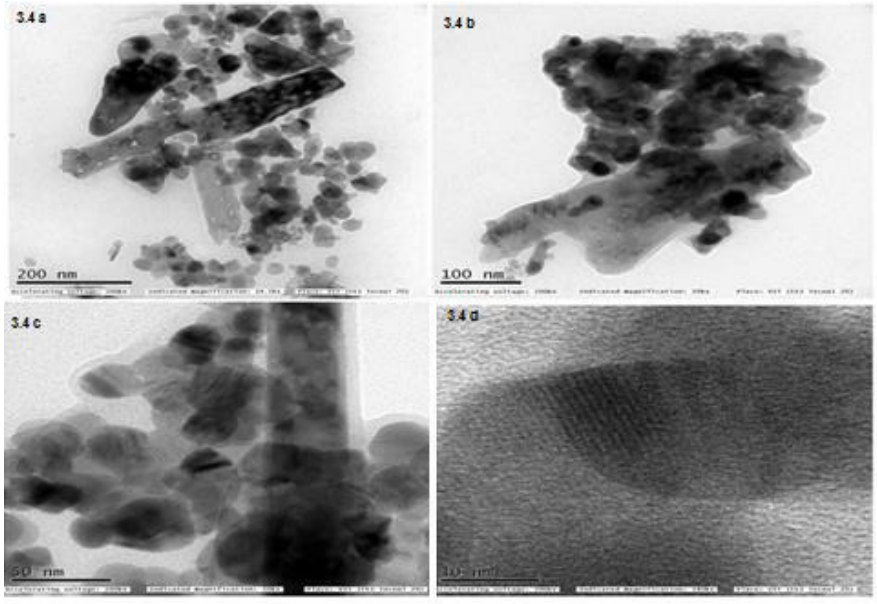

Fig 3.4(a) 200 nm (b) 100 nm (c) 50 nm and (d) 10 nm views of TEM image 8 wt% CdS/Mn-doped ZnO binary nanospheres

3.1.5. Diffused Reflectance UV-Visible analysis of the photocatalyst

UV-visible diffused reflectance spectra of ZnO, Mn doped ZnO nanopowder and various weight ratios of CdS coupled Mn doped ZnO nanospheres were given in Fig 3.5**.** This UV-visible diffuse reflectance spectral study was done for the CdS effect on the optical properties of Mn doped ZnO nanopowder. The light absorbance of pure ZnO only exhibited in the fundamental absorption band in the UV region (397 nm), and the remains absorption band is zero in the visible region. Mn doped ZnO nanopowder (0.007 mol %) slightly shifted the absorption band in the red region, which indicates the band gap reduction than the pure ZnO. In the case of CdS coupled Mn-doped ZnO nanosphere samples significantly enhances the visible light absorption than 0.007 mol% Mn doped ZnO and pure ZnO. [41] It could be revealed that, the CdS coupled Mn-doped ZnO nanospheres and enhances the utilization ability of visible light to improve the photocatalytic activity, which could be attributed to the presence of CdS. Hence, it was consistent with the results of XRD and SEM-EDS, that the UV–vis DRS spectra, which proved the preparation of the CdS coupled Mn-doped ZnO nanosphere is successful. In addition, 8 wt% CdS/Mn codoped ZnO nanospheres had strongest absorption in the visible light, indicating that, it exists in optimal molar ratio of Mn doped ZnO to CdS making the highest photocatalytic activity of CdS/Mn codoped ZnO nanospheres. Simultaneously, the

absorption abilities of 10 wt% CdS/Mn codoped ZnO nanospheres in visible range were significantly lower than that of 8 wt% sample, which could be ascribed to the excessive amount of CdS coupled on Mn doped ZnO surface. It is indicating does not separate the photogenerated e^--h^+ pairs efficiently, which leads to photocatalytic activity decreases. According to the Kubelka-Munk function [42] and plot of (α hv)2 vs. hv, the calculated band gap of ZnO, Mn doped ZnO and CdS are 3.22 eV and 3.18 eV and 2.39 eV respectively

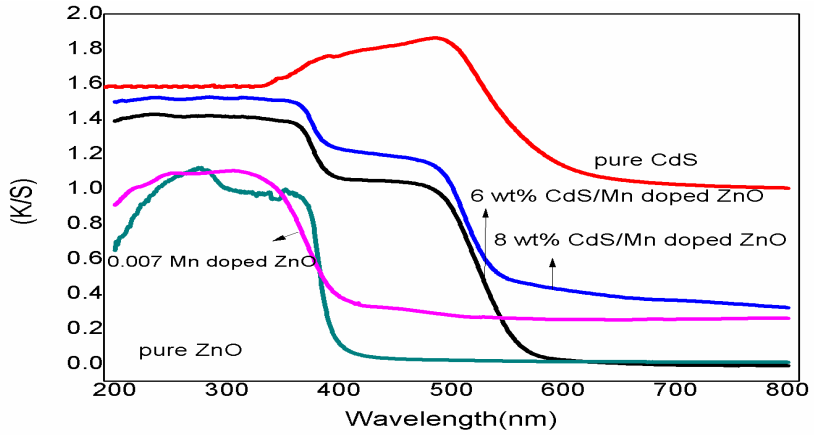

Fig 3.5UV-visible DRS ofnano ZnO, pure CdS, 0.007 mol% Mn- doped ZnO nanopowder, 8 wt% CdS/Mn-doped ZnO and 10 wt% CdS/Mn-doped ZnO binary nanospheres

3.1.6 Photoluminescence study

To exhibit the proposed photocatalytic mechanism, we have measured the photoluminescence behavior of the photocatalyst system. Photoluminescence has been widely employed in the field of photocatalysis over solid semiconductor as a useful probe for understanding the efficiency of charge-carrier trapping, immigration and transfer, and to understand the recombination processes of photo generated electron (e^-)–hole (h^+) pairs.[43] Fig 3.6shows the photoluminescence (PL) emission spectra of nano ZnO, 0.007 mol% Mn- doped ZnO Nano powder and 8 wt% CdS/Mn-doped ZnO binary nanospheres. ZnO has a peak at 578nm in the PL spectrum which corresponds to the recombination of the electron (e^-) and hole (h^+) formed. The emission is significantly weakened largely in the CdS/Mn-doped ZnO binary nanospheres.

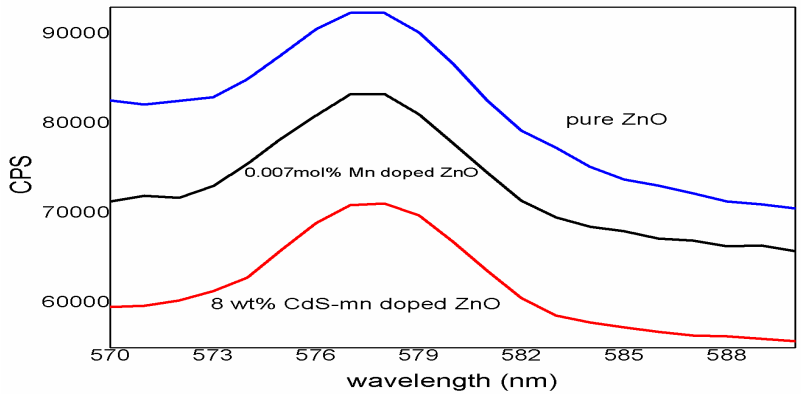

Fig 3.6photoluminescence (PL) emission spectra of nano ZnO, 0.007 mol% Mn- doped ZnO nanopowder and 8 wt% CdS/Mn-doped ZnO binary nanospheres

The observable lower PL intensity at 578 nm implies that the recombination of charge-carriers is effectively inhibited, which probably leads to a higher photocatalytic activity since the photodegradation reactions are induced by these carriers.[44] This result demonstrates good agreement with the proposed mechanism of efficient separation of charge-carriers, as discussed above.

3.2 Photocatalytic *Studies*

3.2.1 Effect *of Catalyst Loading*

The amount of catalyst is one of the main parameters for the degradation studies. In order to avoid the use of excess catalysts it is necessary to find out the optimum loading for efficient removal of dye molecule.[45] Several authors have investigated the reaction rate as a function of catalyst loading in the photocatalytic degradation process. The effect of the catalyst amount on the photocatalytic degradation MB has been carried out in the range 25- 150 mg/L of the CdS/Mn-doped ZnO binary nanospheres for 50 ml of 20 mg solution and these results are shown in Fig 3.7. As the amount of the catalyst is increased from 25 to 100 mg, the degradation increases like19.57 to 88.88 % at 60 min of irradiation time. This is due to an increase in the number of CdS/Mn-doped ZnO binary nanospheres, which increases the absorption of photons and adsorption of dye molecules.

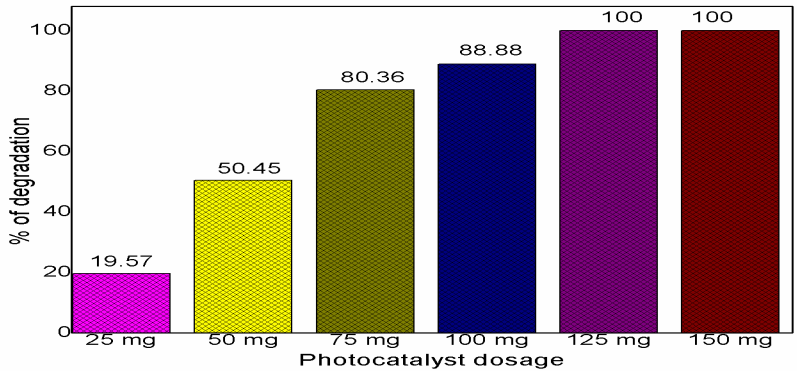

Fig 3.7Effect of initial concentration of MB on the photocatalytic process of CdS/Mn-doped ZnO binary nanospheres

3.2.2 *Effect of pH of the dye solution on CdS/Mn-doped ZnO binary nanospheres*

The pH of solutions greatly affects the rate of reaction taking place on semiconductor surface due to its influences on surface-charge-properties of the photocatalysts.

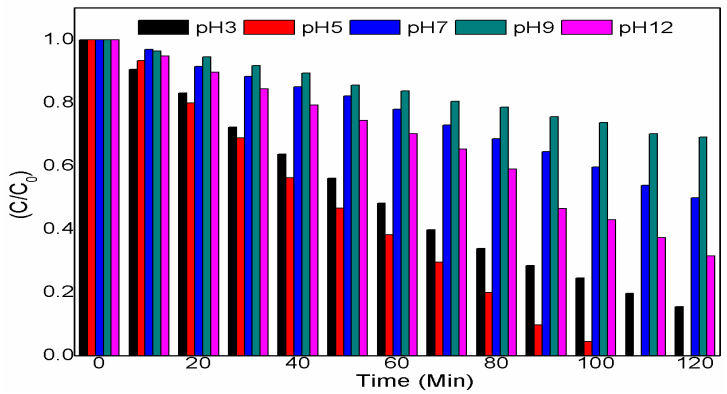

Fig 3.8 Effect of pH of the dye solution on CdS/Mn-doped ZnO binary nanospheres

Fig 3.8**,** shows the photodegradation of MB in the presence of CdS/Mn-doped ZnO binary nanospheres was studied in the pH range 3-12. The concentration of dye solution was 20 mg/L, and the dosage of the photocatalyst was 0.5 mg. Therefore, in the pH range 7-9 the negatively charged CdS/Mn-doped ZnO binary nanospheres and the positive charge MB dye should readily attracts each other, while they should repulse each other when pH is below, 7 due to both species like MB dye and CdS/Mn-doped ZnO binary nanospheres shows positive charge. The degradation rate of CdS/Mn-doped ZnO binary nanospheres was high at around pH 9. The ultimate reason is semiconductor photocatalysts are negatively charged at pH above 7 and the MB has been positively charged species. [46] The ZnO based nanocomposites at extreme pH values, such as pH 3 and 12getreadily dissolved. In an acidic and basic environment, ZnO photocatalyst reveal a propensityto dissolve:

$$ZnO + 2H^{+} \longrightarrow Zn^{2+} + H_2O$$

$$ZnO + H_2O + 2OH^{-} \longrightarrow Zn(OH)_4^{2-}$$

Therefore, the decreased photocatalytic activity at low and higher pH values can be attributed to the dissolution in strong acidic or alkaline environment.

3.2.3 *Photodegradability of methylene blue*

Photocatalysis has become one of the most gifted technologies, due to its potential applications in solar energy conversion to solve the worldwide energy scarcity and environmental pollution.[47] As is well known, solar light is an unlimited supply of energy in nature. There is only a small portion (4%) of solar radiation in the UV region, while visible light is far more abundant (>46%), thus enhancing the photocatalytic capability of semiconductors under visible light as well as UV light irradiation has become an necessary issue in order to highly utilize solar energy. In this work, MB with a characteristic absorption at 668 nm, is chosen as a typical dye pollutant for testing the photocatalytic activity of the as-prepared products under solar light irradiation. Fig. 3.9(a) shows the instantaneous MB concentrations variations versus time in the presence of CdS/Mn-doped ZnO binary nanospheres. The graphs in the first 20 min before light irradiation are caused by the MB adsorption-desorption process onthe catalyst surfaces. It can be seen that only ~10% decrease in the concentration of MB can be observed in the presence of ZnO based photocatalyst.The optimized 0.007

mol% Mn doped ZnO nanopowder was further evaluated the dye degradation, ability when modified with different weight content of CdS with Mn doped ZnO under the solar light irradiation.After 60 min of solar light illumination, the MB degraded over CdS, ZnO and 0.007mol% Mn doped ZnO nanopowder are only 20%, 23%, 29% respectively. However, CdS/Mn-doped ZnO binary nanospheres shows higher photocatalytic degradation rate(76-99%) in the presence of same experimental conditions. It is worth noting that CdS coated Mn-doped ZnO nanopwder could be inducing notable photodegradation efficiency from 80% to 98% beyond the increases of 8 wt % of CdS. From the results, the photocatalytic activity of 0.007 mol% Mn doped ZnO nanopowder increases with the increase in CdS content 2 wt% to 8 wt % due to the tightly bonded or close contact interfaces between CdS and Mn-doped ZnO, by which the injection of photogenerated electron of CdS transfer of conduction band of Mn-doped ZnO and also absorbs visible light. On the contrary, when the mass ratio was higher than 8 wt%, the CdS got agglomerated and it was not well dispersed. This hinders the smooth contact between Mn-doped ZnO systems and CdS, leading to a negative influence on the activity of the 10 wt % CdS/Mn-doped ZnO binary nanospheres. The studies also show that photoelectron injector, such as CdS has very low photocatalytic activity in UV-visible light (solar light) when compared to that of Mn-doped ZnO and ZnO photocatalysts. This shows that the CdS has a smaller electron-hole diffusion length than the W,N codoped ZnO and ZnOphotocatalysts.The kinetics of degradation of MB dye over ZnO, Mn-doped ZnOandCdS/Mn-doped ZnO binary nanosphereshas been studied in natural sunlight. The normalized C/C_0 Vs time plots for the dyes were given in Fig 3.9b**.** The data were also analysed with the Langmuir–Hinshelwood kinetic model:

$$r = \left(\frac{kKC}{1 + KC} \right)$$

Where r is the specific degradation reaction rate the dye ($mgl^{-1}min^{-1}$), C the concentration of the dye ($mg\ l^{-1}$), k the reaction rate constant (s^{-1}) and K is the dye adsorption constant. When the concentration (C) is small enough, the above equation can be simplified in an apparent first-order equation:[48]

$$\left(-\frac{dC}{dt} \right) = r = kKC = k_{app}C$$

After integration, we will get

$$-\ln\left(\frac{C}{C_0} \right) = k_{app}\, t$$

Where C_0 is the initial concentration ($mg\ l^{-1}$), C is the concentration of the dye after t minutes of illumination and k_{app} is the apparent first order rate constant. The plots obtained were shown as Fig 3.9 **b.** The photocatalytic degradation of MB dye on CdS/Mn-doped ZnO binary nanospheres was found to be faster than that of the pure ZnO and Mn- doped ZnO. The CdS/Mn-doped ZnO binary nanospheres shows higher activity than the Mn-doped ZnO and pure ZnO, the reason is due its band gap difference. [49]

Fig 3.9 a

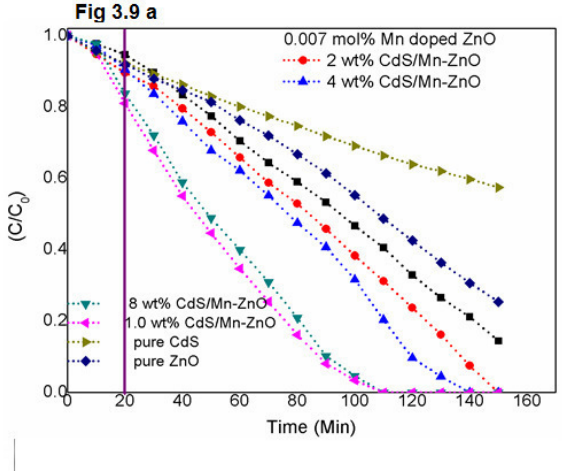

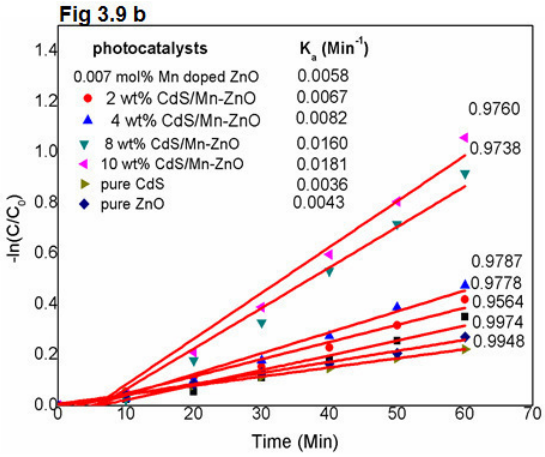

Fig 3.9 a) degradation b) Kinetics of MB dyeover CdS/Mn-doped ZnO binary nanospheres (initial concentration C_0 = 50 mgl^{-1})

3.2.4 *Photocatalytic Mechanism*

The work mechanism of these CdS/Mn-doped ZnO binary nanospheres is illustrated in **Fig 3.10**. The CdS as an electron donor can inject the e- on conduction band of Mn-doped ZnO and which process compeciate the electron for the recombination in the UV-visible photoexcitation of Mn-doped ZnO. This function of CdS can promote the decomposition of organic pollutants under the oxidation of the H^+ by Mn-Mn-doped ZnO.

doped ZnO. The applications conversing this principle, namely organic compounds as the H^+ scavenger for the elimination of selenite pollutants, have been extensively studied. Then, CdS, can deposit onto Mn-doped ZnO and shift the absorbency of the system to the visible light region due to CdS narrowband gap 2.59 eV. [50] Thus, the 10 wt % CdS/Mn-doped ZnO binary nanospheres is a hopeful form for further improving the practicability of CdS and

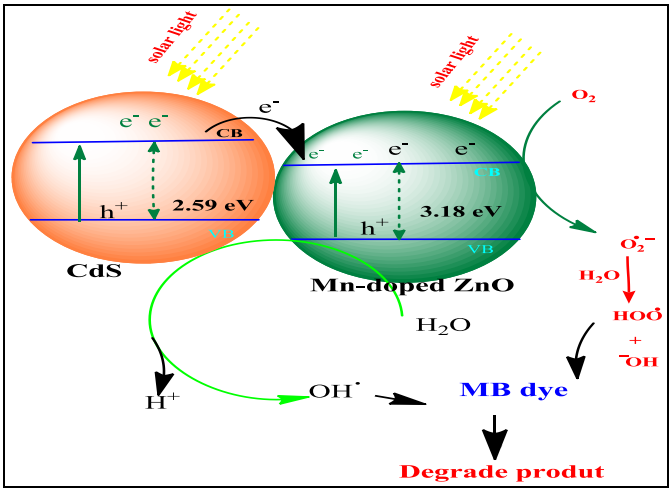

Fig 3.10 Photocatalytic mechanism of prevention of electron-hole recombination and electron injection process of CdS/Mn-doped ZnO binary nanospheres

3.2.5 *Role of Reactive Species*

Fig 3.11 shows the photocatalytic degradation results in the presence of different scavengers under sunlight irradiation. The degradation efficiency of MB decreased slightly upon in presence of AO compared with the without scavenger, which indicated the photogenerated holes are not the main active species for degradation of MB dye. When BQ was added to the photocatalytic mixture, a dramatic change in the

photocatalytic activity was observed compared with the absence of scavenger, confirming that the dissolved oxygen (O^{2-}) has a main source on the photodegradation process under sunlight irradiation. However, a similar change in the photocatalytic activity was observed upon the addition of IPA as a ·OH scavenger, which indicates that the O^{2-} and ·OH are the main reactive species in the CdS/Mn-doped ZnO binary nanospheres[51,52].

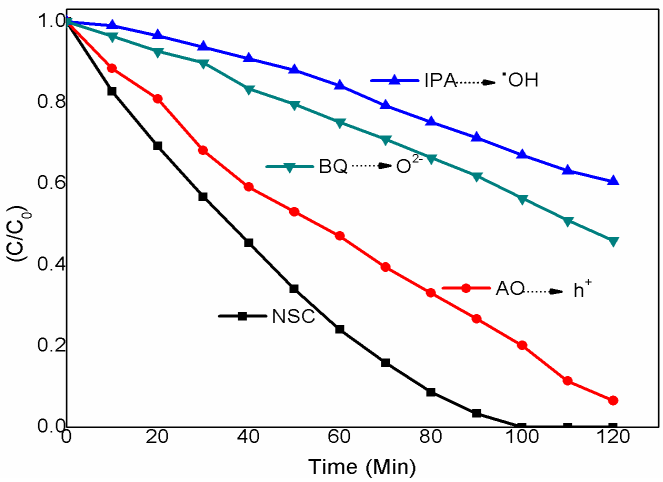

Fig 3.11 Effect of different scavengers on degradation of MB dye in the presence of CdS/Mn-doped ZnO binary nanospheres under solar light irradiation

3.2.6 *Stability and Reusability*

In order to evaluate the stability of CdS/Mn-doped ZnO binary nanospheres during photocatalytic reaction, cycling experiments were also carried out by repeated degradation of MB dye for five times under solar light irradiation. As shown in Fig. 3.12, the photocatalytic activity of CdS/Mn-doped ZnO binary nanospheres is high even with third cycles. Further, the degradation rate was slight decrease, which could be due to the loss and catalytic poisoning of the photocatalyst during the recycling experiments.[53]

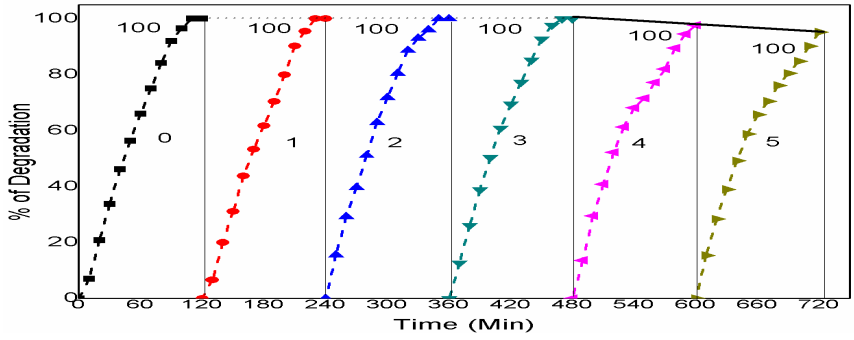

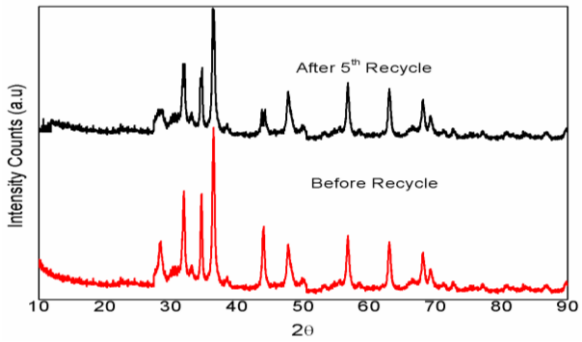

Fig 3.12(a) Stability test of CdS/Mn-doped ZnO binary nanospheres for five cycles and (b) XRD pattern for CdS/Mn-doped ZnO binary nanospheres before the activity and after recycling five times for RB 5 degradation. Fig 3.12 shows the XRD patterns of the CdS/Mn-doped ZnO binary nanospheres before and after photocatalytic reaction, and there is no observable structural difference in the samples before and after the reaction, indicating that the phase and structure of CdS/Mn-doped ZnO binary nanospheres are stable during the photocatalytic reactions. [54]But the intensity of main diffraction pattern decreased due to accumulation of degraded intermediates. These results indicate that the as prepared ternary photocatalyst are stable and reusable for photocatalytic reactions.

3.2.7 *Model Pollutant (dye) degradation behavior from the various water samples*

The selected 8 wt % Mn-doped ZnO nanospheres were applied to remove MB dye (model pollutant) from various types of water. [55-57]For this purpose, water samples were taken from four different sources. The tap water was taken from my own house Salem, distilled water was purchased in Mercury scientific company, Salem and the seawater sample was taken from the Mettur Dam, Salem, while the sea water

from Merina beach Chennai. The MB dye was added to the water sample to make the solutions of almost same concentration (0.05 g). To study the dye degradation behavior of various water samples, the CdS/Mn-doped ZnO binary nanospheres was added (10 ppm) in the presence of sunlight. The Fig. 3.13 shows the degradation behavior of the MB dye in various water samples. Fig. 12 shows that fastest degradation occurred in DI water (100%) and then respectively in river water (~80 %), tap water ((~680 %) and sea water (~20 %). This delay in degradation process may be due to presence of various elements.

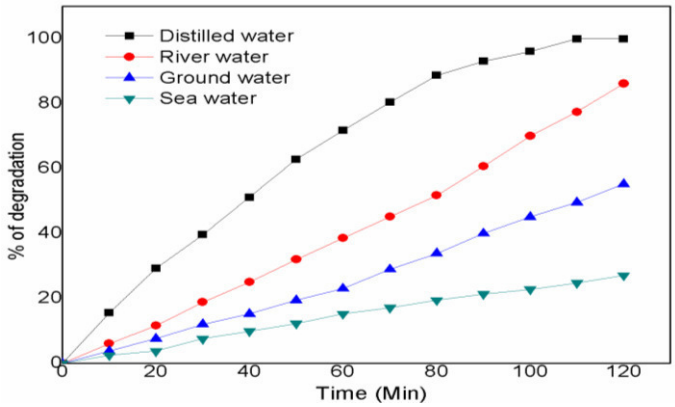

Fig 3.13Pollutant (dye) degradation behavior from the various water samples.

4. CONCLUSION

In this paper, CdS/Mn-doped ZnO binary nanospheres were effectively synthesized with a simple ethanolic dispersion method followed by annealing at 300 °C for 3 hr. The characterization of the photocatalysts was done by XRD, SEM, TEM, EDX, UV-visible and PL spectroscopy. The comparative photocatalytic degradation revealed the excellent photocatalytic efficiency of CdS/Mn-doped ZnO binary nanospheres, compared to Mn-doped ZnO, pure ZnO and CdS samples, and it degraded 100% of MB in 90 minutes under sunlight illumination. Furthermore, the energy band positions of CdS and Mn-doped ZnO are well-matched, leading to further enhancement in the charge transfer and separation. Moreover, the active spices experiments (scavenging activity) exposed that the main active species such asO_2^{2-} and •OH. Reuse experiments indicate the reusability and stability of ternary CeO_2/$FeTiO_3$/TiO_2composites and this good characteristic behavior were addressed by XRD analysis. Further, the photocatalytic performances were also tested in the various sources of water with dye. This study introduces a potential new family of novel solar active photocatalysts for degradation of reactive dyes.

5. AUTHOR CONTRIBUTION STATEMENTS

Dr. J.Dharmaraja designed the research work and Ph.D research scholar K. sivaranjani performed the experiments, derived the models and analyzed the data with help of Dr. S.Sivakumar and Dr.J.Dharmaraja. Dr.S. sivakumar assisted with spectral characteristics and dye degradation measurements and K. Sivaranjani helped carry out the characterization of all the samples. Dr. S.Sivakumar and Dr.J.Dharmaraja wrote the manuscript in consultation with K.Sivaranjani.

6. FUNDING ACKNOWLEDGEMENT

We could not receive fund from any government and other funding agencies.

7. CONFLICT OF INTEREST

Conflict of interest declared none.

8. REFERENCES

1. Rajasulochana P, Preethy V. Comparison on efficiency of various techniques in treatment of waste and sewage water – A comprehensive review. Resour Effic Technol. 2016;2(4):175-84. doi: 10.1016/j.reffit.2016.09.004.
2. Yang T, Yu D, Wang D, Yang T, Li Z, Wu M et al. Accelerating Fe(Ⅲ)/Fe(Ⅱ) cycle via Fe(Ⅱ) substitution for enhancing Fenton-like performance of Fe-MOFs. Appl Catal B. 2021;286:119859. doi: 10.1016/j.apcatb.2020.119859.
3. Yu D, Wang L, Yang T, Yang G, Wang D, Ni H et al. Tuning Lewis acidity of iron-based metal-organic frameworks for enhanced catalytic ozonation. Chem Eng J. 2021;404:127075. doi: 10.1016/j.cej.2020.127075.
4. Rajeev B, Yesodharan S, Yesodharan EP. Application of solar energy in wastewater treatment: photocatalytic degradation of α-methylstyrene in water in presence of ZnO. J Water Process Eng. 2015;8:108-18. doi: 10.1016/j.jwpe.2015.09.005.
5. Rauf MA, Ashraf SS. Fundamental principles and application of heterogeneous photocatalytic degradation of dyes in solution. Chem Eng J. 2009;151(1-3):10-8. doi: 10.1016/j.cej.2009.02.026.

6. Matthews RW. Photo-oxidation of organic material in aqueous suspensions of titanium dioxide. Water Res. 1986;20(5):569-78. doi: 10.1016/0043-1354(86)90020-5.
7. LuM, PichatP. Photocatalysis and Water Purification: from Fundamentals to Recent Applications. John Wiley & Sons. 2013.
8. Ollis D, Pichat P, Serpone N. TiO2 photocatalysis-25 years. Appl Catal B. 2010;99(3-4):377. doi: 10.1016/j.apcatb.2010.06.030.
9. Ali N, Awais, Kamal T, Ul-Islam M, Khan A, Shah SJ et al. Chitosan-coated cotton cloth supported copper nanoparticles for toxic dye reduction. Int J Biol Macromol. 2018;111:832-8. doi: 10.1016/j.ijbiomac.2018.01.092, PMID 29355628.
10. Kamal T, Ahmad I, Khan SB, Asiri AM. Bacterial cellulose as support for biopolymer stabilized catalytic cobalt nanoparticles. Int J Biol Macromol. 2019;135:1162-70. doi: 10.1016/j.ijbiomac.2019.05.057, PMID 31145951.
11. Khan MSJ, Kamal T, Ali F, Asiri AM, Khan SB. Chitosan-coated polyurethane sponge supported metal nanoparticles for catalytic reduction of organic pollutants. Int J Biol Macromol. 2019;132:772-83. doi: 10.1016/j.ijbiomac.2019.03.205, PMID 30928377.
12. Shukla BK, Rawat S, Gautam MK, Bhandari H, Garg S, Singh J. Photocatalytic degradation of orange G dye by using bismuth molybdate: photocatalysis optimization and modeling via definitive screening designs. Molecules. 2022;27(7):2309. doi: 10.3390/molecules27072309, PMID 35408707.
13. Hong W, Li C, Tang T, Xu H, Yu Y, Liu G et al. The photocatalytic activity of the SnO2/TiO2/PVDF composite membrane In rhodamine b degradation. New J Chem. 2021;45(5):2631-42. doi: 10.1039/D0NJ04764C.
14. Han L. et al., Eco-friendly preparation of hierarchically selfassembly porous ZnO nanosheets for enhanced photocatalytic performance. SuB, ZhongM. Mater Res Bull. 2020;124:110777-81.
15. Rahman QI, Ahmad M, Misra SK, Lohani M. Effective photocatalytic degradation of rhodamine b dye by ZnO nanoparticles. Mater Lett. 2013;91:170-4. doi: 10.1016/j.matlet.2012.09.044.
16. Wentao Y, Yu J, Qi L, Doudou X, Z, XinWei C et al. The preparation of visible light-driven ZnO/Ag2MoO4/Ag nanocomposites with effective photocatalytic and antibacterial activity. J Alloys Compd. 2021;891:161898.
17. Shwetha Priyadharshini S, Shivalingappa PS J. J, Syed Farooq A, Mufsir K, Mohammad Rafe H, Baji S and Kiran K. Photocatalytic Degradation of Methylene Blue and Metanil Yellow Dyes Using Green Synthesized Zinc Oxide (ZnO) Nanocrystals. Crystals. 2022;12(22):1-16.
18. Jayanta B, Archana D, Bapan B, et al. Optimizing ZnO/CdS nanocomposite controlled by Fe doping towards efficiency in water treatment and antimicrobial activity. Curr World Environ. 2021;16(3).
19. Qamar MA, Shahid S, Javed M, Sher M, Iqbal S, Bahadur A et al. Fabricated novel g-C3N4/Mn doped ZnO nanocomposite as highly active photocatalyst for the disinfection of pathogens and degradation of the organic pollutants from wastewater under sunlight radiations. Colloids and Surfaces A: Physicochemical and Engineering Aspects. 2021;611. doi: 10.1016/j.colsurfa.2020.125863.
20. Neena D, Humayun M, Zuo W, Liu CS, Gao W, Fu DJ. Hierarchical heteroarchitectures of in-situ g-C3N4 - coupled Fe-doped ZnO micro-flowers with enhanced visible-light photocatalytic activities. Appl Surf Sci. 2020;506(15):145017.
21. Zirak M, Moradlou O, Bayati MR, Nien YT, Moshfegh AZ. On the growth and photocatalytic activity of the vertically aligned ZnO nanorods grafted by CdS shells. Appl Surf Sci. 2013;273:391-8. doi: 10.1016/j.apsusc.2013.02.050.
22. Khanchandani S, Kundu S, Patra A, Ganguli AK. Shell thickness dependent photocatalytic properties of ZnO/CdS core–shell nanorods. J Phys Chem C. 2012;116(44):23653-62. doi: 10.1021/jp3083419.
23. Zirak M, Akhavan O, Moradlou O, Nien YT, Moshfegh AZ. Vertically aligned ZnO@CdS nanorod heterostructures for visible light photoinactivation of bacteria. J Alloys Compd. 2014;590:507-13. doi: 10.1016/j.jallcom.2013.12.158.
24. Jana TK, Pal A, Chatterjee K. Self assembled flower like CdS–ZnO nanocomposite and its photo catalytic activity. J Alloys Compd. 2014;583:510-5. doi: 10.1016/j.jallcom.2013.08.184.
25. Liu C, Yang B, Chen J, Jia F, Song S. Synergetic degradation of methylene blue through photocatalysis and fenton reaction on two-dimensional molybdenite-Fe. J Environ Sci (China). 2022;111:11-23. doi: 10.1016/j.jes.2021.03.001, PMID 34949341.
26. Medhat A, El-Maghrabi HH, Abdelghany A, Abdel Menem NM, Raynaud P, Moustafa YM, et al. Efficiently activated carbons from corn cob for methylene blue adsorption. Applied Surface Science Advances. 2021;3:100037. doi: 10.1016/j.apsadv.2020.100037.
27. Tantawy HR, Nada AA, Baraka A, Elsayed MA. Novel synthesis of bimetallic Ag–Cu nanocatalysts for rapid oxidative and reductive degradation of anionic and cationic dyes. Applied Surface Science Advances. 2021;3:100056. doi: 10.1016/j.apsadv.2021.100056.
28. J P, Kottam N, A R. Investigation of photocatalytic degradation of crystal violet and its correlation with bandgap in ZnO and ZnO/GO nanohybrid. Inorg Chem Commun. 2021;125:108460. doi: 10.1016/j.inoche.2021.108460.
29. Yulizar Y, Eprasatya A, Bagus Apriandanu DOB, Yunarti RT. Facile synthesis of ZnO/GdCoO3 nanocomposites, characterization and their photocatalytic activity under visible light illumination. Vacuum. 2021;183:109821. doi: 10.1016/j.vacuum.2020.109821.
30. Kumar R, Umar A, Kumar R, Chauhan MS, Al-Hadeethi Y. ZnO-SnO2 nanocubes for fluorescence sensing and dye degradation applications. Ceram Int. 2021;47(5):6201-10. doi: 10.1016/j.ceramint.2020.10.198.
31. Beura R, Pachaiappan R, Paramasivam T. Photocatalytic degradation studies of organic dyes over novel Ag-loaded ZnO-graphene hybrid nanocomposites. J Phys Chem Solids. 2021;148:109689. doi: 10.1016/j.jpcs.2020.109689.
32. Park JK, Rupa EJ, Arif MH, Li JF, Anandapadmanaban G, Kang JP. et al. Synthesis of zinc oxide nanoparticles from Gynostemma pentaphyllum extracts and assessment of photocatalytic properties through malachite green dye decolorization under UV

illumination-A Green Approach. Optik. 2021;239:166249. doi: 10.1016/j.ijleo.2020.166249.
33. Nadeem MS, Munawar T, Mukhtar F, Naveed ur Rahman MNU, Riaz M, Iqbal F. Enhancement in the photocatalytic and antimicrobial properties of ZnO nanoparticles by structural variations and energy bandgap tuning through Fe and Co Co-doping. Ceram Int. 2021;47(8):11109-21. doi: 10.1016/j.ceramint.2020.12.234.
34. Yang Y, Wu Z, Yang R, Li Y, Liu X, Zhang L et al. Insights into the mechanism of enhanced photocatalytic dye degradation and antibacterial activity over ternary ZnO/ZnSe/MoSe2 photocatalysts under visible light irradiation. Appl Surf Sci. 2021;539:148220. doi: 10.1016/j.apsusc.2020.148220.
35. Divya G, Sivakumar S, Sakthi D, Priyadharsan A, Arun V, Kavitha R et al. Developing the NiO/CuTiO3/ZnO Ternary Semiconductor Heterojunction for Harnessing Photocatalytic Activity of Reactive Dye with Enhanced Durability. J Inorg Organomet Polym. 2021;31(12):4480-90. doi: 10.1007/s10904-021-02068-0.
36. Divya G, Sakthi D, Priyadharsan A, Boobas S, Sivakumar S. Anatomy of a natural sunlight driven CdS/CoTiO3/ZnO ternary photocatalyst for efficient optical properties and removal of reactive orange 30. Res J Chem Environ. 2021;25(8):100-9. doi: 10.25303/258rjce100109.
37. Sivakumar S, Selvaraj A, Ramasamy AK. Photocatalytic degradation of organic reactive dyes over MnTiO3/TiO2 heterojunction composites under UV-visible irradiation. Photochem Photobiol. 2013;89(5):1047-56. doi: 10.1111/php.12136, PMID 23848842.
38. Tang X, Hu KA. The formation of ilmenite FeTiO3 powders by a novel liquid mix and H2/H2O reduction process. J Mater Sci. 2006;41(23):8025-8. doi: 10.1007/s10853-006-0908-8.
39. Adegoke KA, Iqbal M, Louis H, Bello OS. Synthesis, characterization and application of CdS/ZnO nanorod heterostructure for the photodegradation of rhodamine b dye. Mater Sci Energy Technol. 2019;2(2):329-36. doi: 10.1016/j.mset.2019.02.008.
40. Tian J, Liu Q, Ge C, Xing Z, Asiri AM, Al-Youbi AO et al. Ultrathin graphitic carbon nitride nanosheets: A low-cost, green, and highly efficient electrocatalyst toward the reduction of hydrogen peroxide and its glucose biosensing application. Nanoscale. 2013;5(19):8921-4. doi: 10.1039/c3nr02031b, PMID 23934305.
41. Coulter J, Birnie D. 'Assessing Tauc Plot Slope Quantification: ZnO Thin Films as a Model System,' Phys. Stat Solid B. 2018;255(3):1-7.
42. Carlsson JM, Hellsing B, Domingos HS, Bristowe PD. Theoretical investigation of the pure and Zn-doped α and δ phases of Bi 2 O 3. Phys Rev B. 2002;65(20):205122. doi: 10.1103/PhysRevB.65.205122.
43. Fang X, Lu G, Mahmood A, Tang Z, Liu Z, Zhang L et al. A novel ternary Mica/TiO2/Fe2O3 composite pearlescent pigment for the photocatalytic degradation of acetaldehyde. Journal of Photochemistry and Photobiology A: Chemistry. 2020;400. doi: 10.1016/j.jphotochem.2020.112617.
44. Dadigala R, Gangapuram BR, Bandi R, Dasari A, Guttena V. Synthesis and characterization of C−TiO2/FeTiO3 and CQD/ C−TiO2/FeTiO3 photocatalysts with enhanced photocatalytic activities under sunlight irradiation. Acta Metall Sin (Engl Lett). 2016;29(1):17-27. doi: 10.1007/s40195-015-0356-z.
45. Reza KM, Kurny ASW, Gulshan F. Parameters affecting the photocatalytic degradation of dyes using TiO2: a review. Appl Water Sci. 2017;7(4):1569-78. doi: 10.1007/s13201-015-0367-y.
46. Fatehah MO, Aziz HA, Stoll S. Stability of ZnO Nanoparticles in Solution. Influence of pH, Dissolution, Aggregation and Disaggregation Effects. j coll sci biotechnol;3(1):75-84. doi: 10.1166/jcsb.2014.1072.
47. Darkwah WK, Oswald KA. Photocatalytic Applications of heterostructure Graphitic carbon nitride: pollutant Degradation, Hydrogen Gas Production (water splitting), and CO2 Reduction. Nanoscale Res Lett. 2019;14(1):234. doi: 10.1186/s11671-019-3070-3, PMID 31300944.
48. Naik B, Parida KM. Solar light active photodegradation of phenol over a FexTi1−xO2−yNy nanophotocatalyst. Ind Eng Chem Res. 2010;49(18):8339-46. doi: 10.1021/ie100889m.
49. Liufu S, Xiao H, Li Y. Investigation of PEG adsorption on the surface of zinc oxide nanoparticles. Powder Technol. 2004;145(1):20-4. doi: 10.1016/j.powtec.2004.05.007.
50. Konstantinou I. Photocatalytic transformation of pesticides in aqueous titanium dioxide suspensions using artificial and solar light: intermediates and degradation pathways. Appl Catal B. 2003;42(4):319-35. doi: 10.1016/S0926-3373(02)00266-7.
51. Sher M, Javed M, Shahid S, Iqbal S, Qamar MA, Bahadur A et al. The controlled synthesis of g-C3N4/Cd-doped ZnO nanocomposites as potential photocatalysts for the disinfection and degradation of organic pollutants under visible light irradiation. RSC Adv. 2021;11(4):2025-39. doi: 10.1039/d0ra08573a, PMID 35424172.
52. Sorathiya K, Mishra B, Kalarikkal A, Reddy KP, Gopinath CS, Khushalani D. Enhancement in rate of photocatalysis upon catalyst recycling. Sci Rep. 2016;6:35075. doi: 10.1038/srep35075, PMID 27731347.
53. Thirumala RG, Ravikumar RVSSN, Ravindranadh K. Enhanced photocatalytic activity of ZnO−CdS composite nanostructures towards the degradation of rhodamine b under solar light. Catalysts. 2022;12(84):1-13.
54. Bibi R, Shen Q, Wei L, Hao D, Li N, Zhou J. Hybrid BiOBr/UiO-66-NH2 composite withenhanced visible-light driven photocatalytic activity toward RhB dye degradation. RSC Adv. 2018;8(4):2048-58. doi: 10.1039/c7ra11500h, PMID 35542604.
55. Muhammad TSC, Sher BK. Mohammed M. Rahman Tahseen K, Abdullah MA, Sunlight assisted photocatalytic dye degradation using zinc and iron based mixed metal-oxides nanopowders. J King Saud Univ Sci. 2022;34:101841.
56. Azeez F, Al-Hetlani E, Arafa M, Abdelmonem Y, Nazeer AA, Amin MO et al. The effect of surface charge on photocatalytic degradation of methylene blue dye using chargeable titania nanoparticles [sci rep]. Sci Rep. 2018;8(1):7104. doi: 10.1038/s41598-018-25673-5, PMID 29740107.

57. Chadwick MD, Goodwin JW, Lawson EJ, Mills PDA, Vincent B. Surface charge properties of colloidal titanium dioxide in ethylene glycol and water. Colloids and Surfaces A: Physicochemical and Engineering Aspects. 2002;203(1-3):229-36. doi: 10.1016/S0927-7757(01)01101-3.